

Rheological heterogeneities at the roots of the seismogenic zone

G. Volpe^{1,*}, G. Pozzi², M.E. Locchi¹, E. Tinti^{1,2}, M.M. Scuderi¹, C. Marone^{1,3}, and C. Collettini^{1,2}¹Dipartimento di Scienze della Terra, La Sapienza Università di Roma, 00185 Rome, Italy²Istituto Nazionale di Geofisica e Vulcanologia, 00143 Rome, Italy³Department of Geoscience, Pennsylvania State University, University Park, Pennsylvania 16802, USA

ABSTRACT

Although rheological heterogeneities are invoked to explain differences in fault-slip behavior, case studies where an interdisciplinary approach is adopted to capture their specific roles are still rare. In this work, we integrated geophysical, geological, and laboratory data to explain how rheological heterogeneities influence the earthquake activity at the roots of the seismogenic zone. During the 2016–2017 Central Italy sequence, following the major earthquakes, we observed a deepening of seismicity within the basement associated with a transient stress change. Part of this seismicity was organized in clusters of events, with similar sizes and waveforms. The structural study of exhumed basement rocks highlighted a heterogeneous fabric made of strong, quartz-rich lenses (up to 200 m) surrounded by a weak, interconnected phyllosilicate-rich matrix. Laboratory experiments simulating the main shock-induced increase in loading rate showed that the matrix lithology experienced an accelerating and self-decelerating aseismic creep, whereas the lens lithology showed dynamic instabilities. Our results suggest that the post-main shock loading rate increases favored accelerated creep within the matrix, which promoted, as a consequence, seismic instabilities within the lenses in the form of clustered seismicity. Our findings emphasize the strong connection between seismicity and the structural and frictional properties of the seismogenic zone.

INTRODUCTION

Geological investigations on exhumed faults and shear zones have defined heterogeneous fault structures (e.g., Fagereng and Sibson, 2010) ranging from localized deformation on one or more discrete planes to distributed deformation within thick shear zones. A common view is that shear localization results from cataclastic processes affecting granular fault rocks, whereas phyllosilicate-rich rocks promote the development of thick and distributed shear zones (e.g., Faulkner et al., 2010; Collettini et al., 2019). The structural heterogeneities described along exhumed faults are strongly connected to frictional heterogeneities. Localized deformation commonly correlates with high friction, $\mu \sim 0.6$, high healing rates, and a rate-weakening behavior (Ikari et al., 2011; Collettini et al., 2019). For these reasons, fault patches with localized deformation are considered strong (high friction), locked (high healing rates), and potentially unstable (rate weakening). On the other hand, distributed frictional sliding along thick phyllosilicate-rich shear zones results in low

friction, $0.1 < \mu < 0.3$, low healing rates, and rate-strengthening behavior, and thus these fault patches are typically weak, favoring stable creep (Ikari et al., 2011; Lockner et al., 2011; Collettini et al., 2019).

More than 30 yr of high-resolution earthquake detection and location have highlighted distinctive features of seismicity that seem to be connected to geological and frictional heterogeneities. Along plate-boundary faults or subduction zones, small earthquakes with identical waveforms have been interpreted as repeated ruptures originating from the same fault patch (Nadeau et al., 1994; Igarashi et al., 2003; Uchida and Bürgmann, 2019). The recurrence time of repeaters as a function of loading rate suggests that repeaters nucleate from discrete structures representing small and locked fault patches (i.e., asperities) loaded by the surrounding fault creep (Uchida and Bürgmann, 2019; Waldhauser et al., 2021). Along intracontinental faults, low loading rates do not allow for long-term (decades) characterization of repeaters. Here, it appears that the activity of repeaters is isolated to shorter intervals, less than 1 mo, and can be related to special conditions such as changes in the loading rate preceding and fol-

lowing large main shocks or transient high fluid pressure (Chiaraluze et al., 2007; Vuan et al., 2017; Uchida and Bürgmann, 2019; Essing and Poli, 2022). Loading by large main shocks can also promote a transient deepening of the base of the seismogenic zone (Ellis and Stöckhert, 2004; Cheng and Ben-Zion, 2019). This provides useful insights on the stress state of the overlying seismogenic zone.

Although field, laboratory, and seismological observations can provide a coherent picture of the ways in which fault heterogeneities may influence slip behavior (Fagereng and Sibson, 2010; Uchida and Bürgmann, 2019; Fagereng and Beall, 2021; Bedford et al., 2022), this picture remains fuzzy because case studies where complementary observations are integrated are still rare. Here, we addressed this gap by studying the 2016–2017 Central Italy seismic sequence. We show that clustered aftershock activity at the base of the seismogenic zone was promoted by the increased loading rates induced by the main shocks within otherwise creeping rock volumes.

RESULTS

Seismicity within the Basement

The 2016–2017 Central Italy seismic sequence started on 24 August 2016 with the Amatrice $M_w = 6.0$ earthquake (Fig. 1A). This first main shock was followed by two other large earthquakes: the $M_w = 5.9$ Visso and $M_w = 6.5$ Norcia earthquakes on 26 and 30 October, respectively. On 18 January 2017, the $M_w = 5.5$ Campotosto earthquake (the largest of four events with $M_w > 5.0$) occurred on the SE portion of the sequence (Fig. 1A). The seismic sequence activated a NW-SE-trending, 80-km-long normal fault system. The base of the seismogenic zone (defined as the depth above which 95% of seismicity occurs; e.g., Sibson, 1989; Magistrale, 2002) is located at ~ 9 km depth, where seismic reflection profiles mark the top of the acoustic basement (Barchi et al., 2021; Volpe et al., 2022). Within the

G. Volpe  <https://orcid.org/0000-0003-0165-0446>
*giuseppe.volpe@uniroma1.it

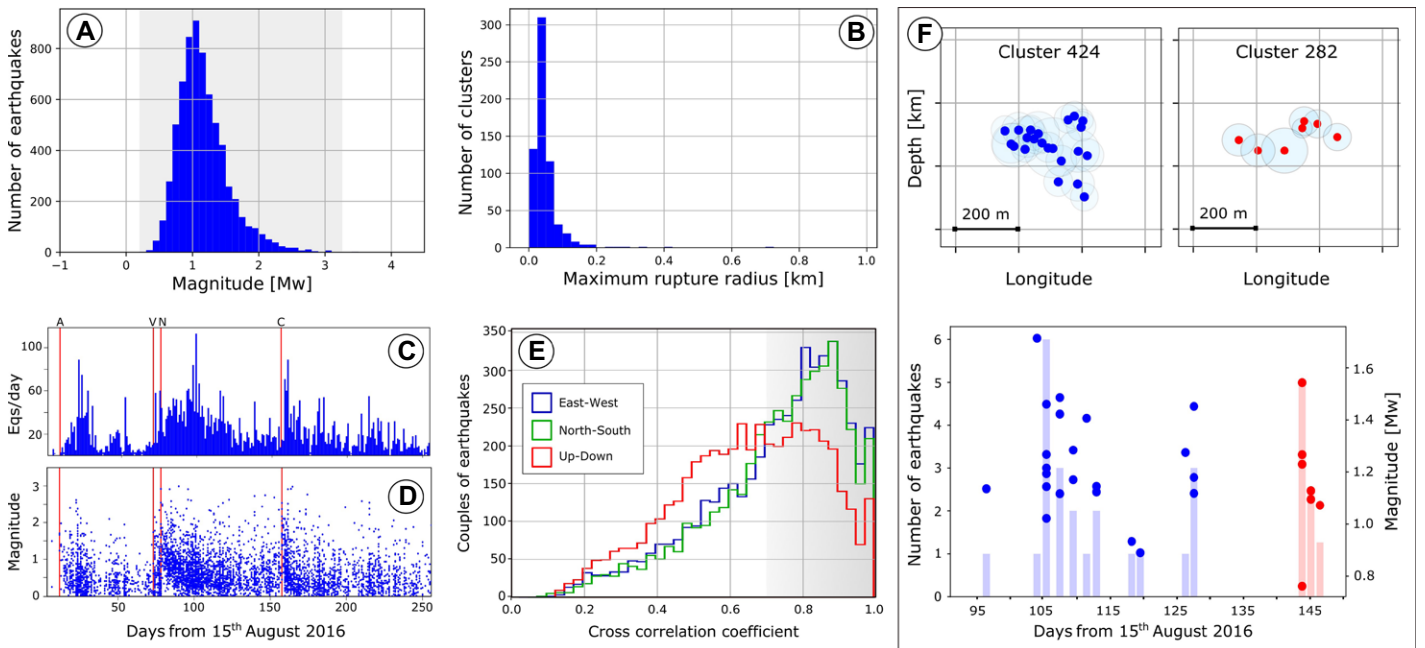
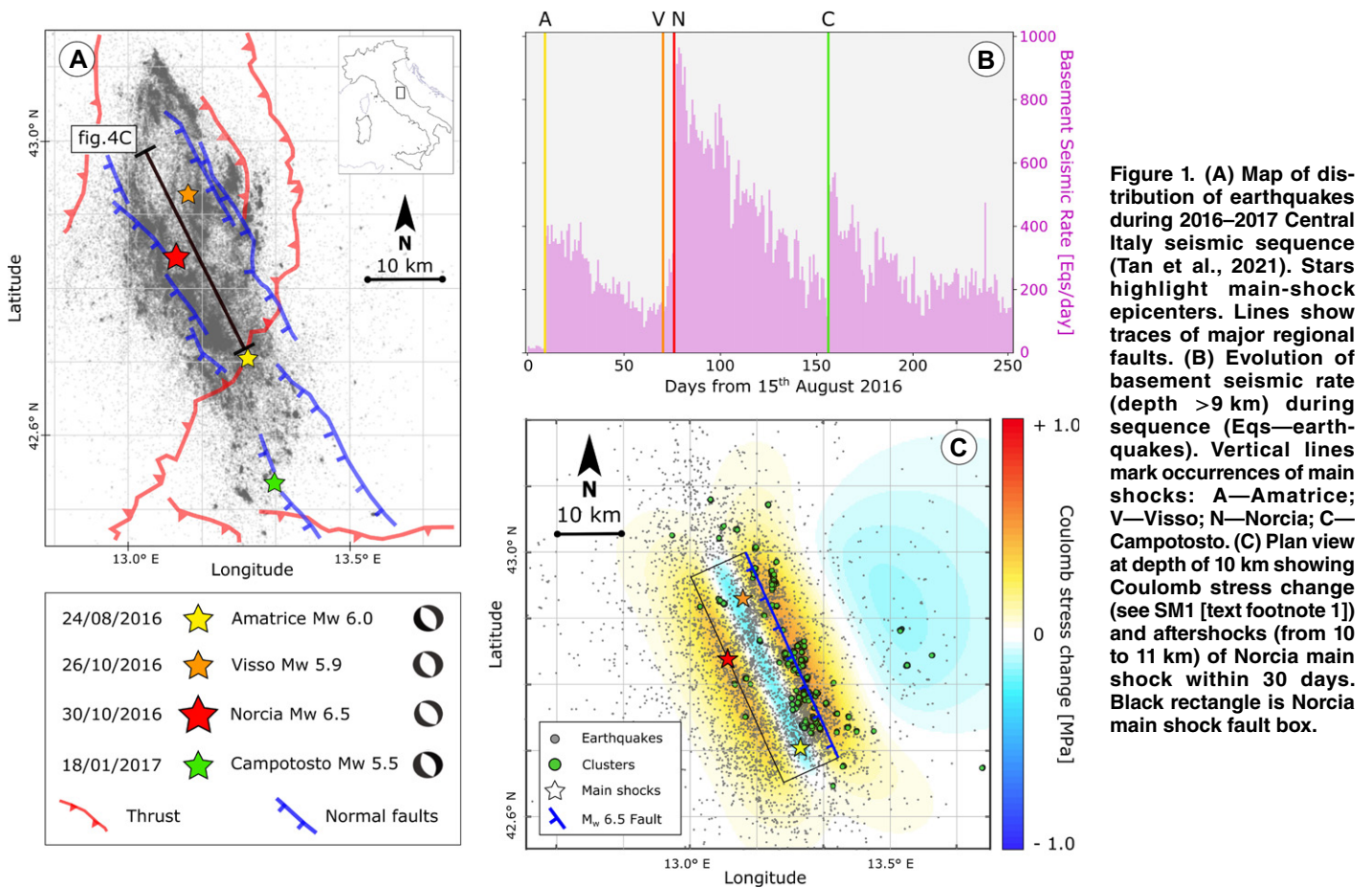


Figure 2. (A) Magnitude distribution of clustered events. **(B)** Distribution of maximum rupture radius for each cluster, considering stress drop of 3 MPa (e.g., Kanamori and Anderson, 1975). **(C)** Daily evolution of cluster seismic rate. Vertical lines mark occurrences of main shocks: A—Amatrice; V—Visso; N—Norcia; C—Campotosto. **(D)** Daily evolution of magnitude of clustered events. **(E)** Cross-correlation coefficient distributions for each seismogram component. **(F)** Cross sections of two clusters (upper panels) with associated rupture radius, number of earthquakes, and magnitude distribution in time (lower panel).

seismogenic zone, seismicity is localized on SW-dipping normal faults hosting the main shocks (e.g., Chiaraluce et al., 2017) and distributed on imbricated bands located between 5 and 9 km depth (SM2 in the Supplemental Material¹). These bands have been variously interpreted as: extensional detachments (Waldhauser et al., 2021), reactivated ancient thrusts (Improta et al., 2019), or distributed deformation favored by a ductile-brittle rheology (Collettini et al., 2022). Below the seismogenic zone, the rheology of the basement is controlled by the rate-strengthening nature of phyllosilicate-rich rocks, promoting a frictionally controlled seismicity cutoff (Volpe et al., 2022; see also SM2) and providing key information to understand the deformation processes at play at the roots of the seismogenic zone.

To gain insight into the deformation processes of the basement, we analyzed the evolution of the basement seismicity in space and time, building on a high-resolution seismic catalogue spanning a 1-yr period (Tan et al., 2021). We observed in the basement an abrupt increase in the seismicity rate (Fig. 1B) immediately after the main shocks ($M_w > 5.5$). Then, the seismicity rate decreased to a sequence background level. Part of the basement seismicity (15%) was organized in 625 small clusters (Fig. 1C) that we highlighted via a spatial-temporal clustering algorithm (SM3) and analyzed in space and time.

While most clusters were sparse, some were instead organized along east-dipping subparallel structures (SM2). All clusters were characterized by earthquakes of small magnitude ($0 < M_w < 3.5$), with a mode of $M_w = 1.1$ (Fig. 2A), corresponding to an average rupture radius < 400 m (Fig. 2B), with a mode of ~ 35 m. The clusters showed short-term activity (< 13 d) with variation of the seismicity rate through time (Fig. 2C). The largest events were homogeneously distributed in time without any correlation with the main shocks (Fig. 2D), consistent with a swarm-like evolution (Vidale and Shearer, 2006). To further explore cluster seismicity, we studied the waveform similarity of the earthquakes within each of 125 randomly selected clusters. This was performed by cross-correlation coefficient (CCC) analysis over long windows, capturing the entire wave train: from the P-wave arrival to 2 s after the S-wave arrival (SM4 and SM5 [see footnote 1]). The mode of the cumulative distribution of all components ranged between 0.8 and 0.9 (Fig. 2E), and $\sim 72\%$ of the clusters were characterized

by more than two events with CCC > 0.9 . Most of the analyzed clusters consisted of more than four spatially separated events, occurring in a short time window, and with partially overlapping source regions (Fig. 2F). These data suggest that the Apenninic basement is structurally complex and composed of small asperities that host swarm-like (i.e., burst-type) earthquakes when subject to main shock-induced stress increases (Figs. 1B and 1C).

Basement Structures and Frictional Properties

Details on the geology of the basement were obtained from both deep boreholes within the seismically active area of the Apennines (Pialli, 1998) and geological outcrops (Volpe et al., 2022; Giuntoli and Viola, 2022). Basement fabric can be described as an interconnected matrix (Figs. 3A and 3B) of highly deformed and foliated phyllosilicate-rich rocks (Fig. 3A) that envelop hundred-meter-wide lenses composed of quartz-rich rocks (Figs. 3A and 3B), the latter populated by veins and faults.

The phyllosilicate-rich rocks have a low friction coefficient ($\mu = 0.28$), low healing rate ($\beta = 0.0002$), and rate-strengthening behavior ($a-b = 0.0034$; Volpe et al., 2022). These rocks are thus weak horizons that can easily creep at the low loading rates of the central Apennines (3 mm/yr; Anderlini et al., 2016). The quartz-rich lenses have higher friction ($\mu = 0.50$), high healing rates ($\beta = 0.0069$), and nearly rate-neutral behavior ($a-b = 0.001$; Volpe et al., 2022); therefore, they represent asperities within the basement. We posit that, following the main shocks, the transient stress increase within the basement (Fig. 1C) produced complex slip behavior controlled by the basement geometry and its frictional properties. To assess this behavior, we performed a suite of laboratory experiments simulating the post-main shock stress rate increase (details in SM6). We tested both phyllosilicate-rich matrix and quartz-rich lenses using three shear-stress rate protocols (Figs. 3E and 3F). We started from a stress level at 80% of the steady-state frictional strength (τ_{ss} , the stress required to reactivate the fault), and we

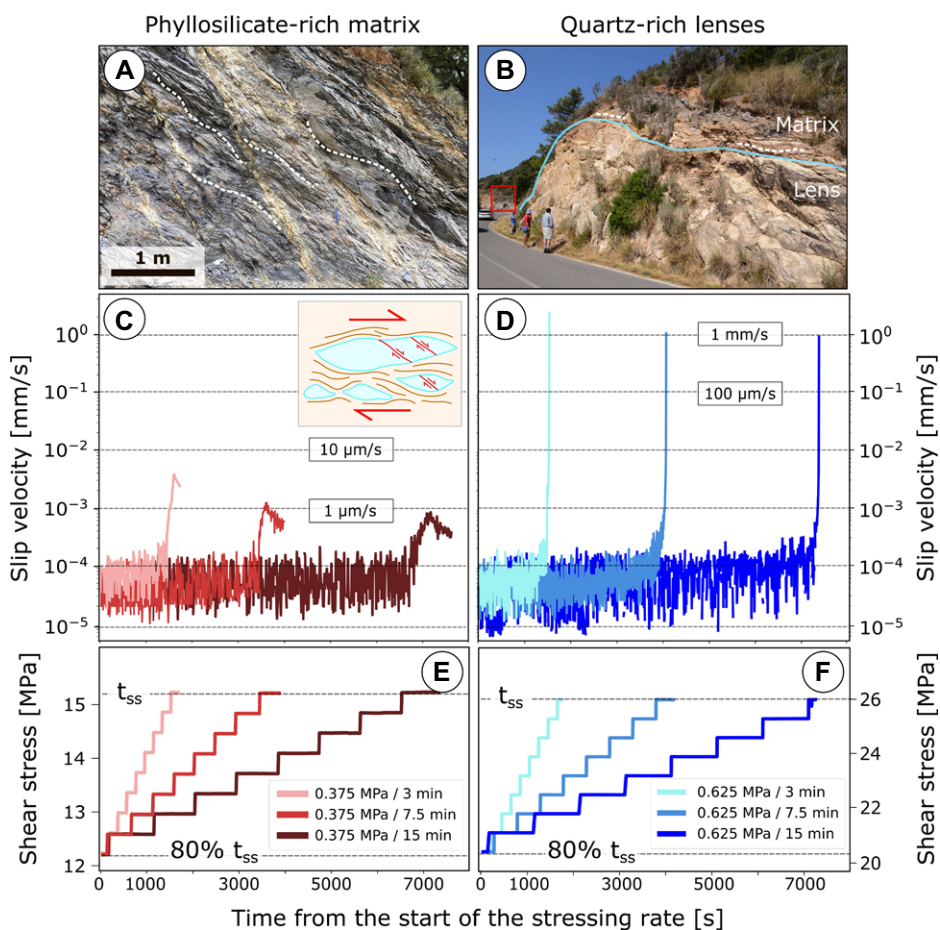


Figure 3. (A–B) Photos of exhumed basement rocks in Mount Argentario (Tuscany, Italy), showing highly deformed matrix characterized by pervasive foliation (marked by dashed white lines) (A), and contact between strong lens and foliated matrix (cyan line) (B). Location of A is marked by red box in B. (C–D) Evolution of slip velocity vs. time for phyllosilicate-rich matrix (C) and quartz-rich lenses (D) for three loading-rate protocols, represented in E and F. (E–F) Three loading-rate protocols. Mineralogy is given in SM7 (see text footnote 1). t_{ss} —steady-state frictional strength.

¹Supplemental Material. SM1 (Coulomb stress change); SM2 (basement geometries); SM3 (clustering methods); SM4 (cross-correlation analysis); SM5 (clusters); SM6 (experimental apparatus and procedures); SM7 (basement gougues); and SM8 (seismicity cutoff evolution). Please visit <https://doi.org/10.1130/GEOLOGY.S23881308> to access the supplemental material, and contact editing@geosociety.org with any questions.

increased the stress stepwise while monitoring the fault-slip behavior (Figs. 3C and 3D). When the shear stress remained below τ_{ss} (Fig. 3), the experimental fault was stable and deformed at creeping velocities of tens of nanometers per second (Figs. 3C and 3D). When the shear stress reached τ_{ss} , we observed different styles of fault reactivation depending on the rock type. The phyllosilicate-rich matrix gently accelerated to a slip velocity (V) of $\sim 1 \mu\text{m/s}$ and then self-decelerated (Fig. 3C). Conversely, the quartz-rich lenses abruptly accelerated to slip velocities higher than millimeters per second (Fig. 3D). Our results suggest that a transient stress increase can result in creep acceleration for both materials, but only the quartz-rich lenses evolve into an earthquake-like instability.

DISCUSSION AND CONCLUSION

Our data provide an integrated view (Fig. 4) on the style of deformation at the roots of the seismogenic zone during the Central Italy 2016–2017 seismic sequence. Following the main shocks, the seismicity significantly increased within the basement (Fig. 1). About 15% of the basement seismicity was organized in small clusters that occurred in crustal volumes loaded by the main shocks (Fig. 1C). The remaining seismicity was homogeneously distributed and could have been due to several factors, including small lenses, earthquakes occurring within the matrix, or earthquakes occurring within small inherited faults. Clusters were generally characterized by short-term activity (<13 d) and low average magnitudes ($M_w \sim 1.1$), and they consisted of events with partially overlapping

source regions (Fig. 2). Outcrops of basement lithologies (Fig. 3), representing exhumed analogues of rocks where clustering activity occurs, show pervasive and distributed deformation along interconnected and phyllosilicate-rich networks (matrix) that surround quartz-rich lenses (hundreds of meters wide) with fractures and localized faults. Laboratory friction experiments with variable loading rates showed that the phyllosilicate-rich rocks deform by an accelerating and self-decelerating aseismic creep, whereas the quartz-rich rocks reactivate via dynamic instabilities.

Our findings provide insights on the mechanisms that control the deepening of the seismogenic zone (e.g., Sibson, 1989; Cheng and Ben-Zion, 2019). The base of the seismogenic zone is generally linked to the brittle-ductile transition (BDT; Brace and Kohlstedt, 1980; Sibson, 1989), and in this view, the BDT divides an upper crust characterized by brittle and seismogenic faults from a lower crust where deformation is accommodated aseismically by viscous shearing in thick quartz-rich mylonites at temperature $>300^\circ\text{C}$ (Brace and Kohlstedt, 1980). In the central Apennines, rheological models building on heat-flow data locate the BDT at ~ 15 km depth for quartz-rich lithologies (Pauselli et al., 2019). However, during the 2016–2017 Central Italy seismic sequence, a marked seismicity cutoff occurred at ~ 9 km depth, corresponding to the phyllitic basement (Fig. 4C; SM2; Volpe et al., 2022). Following the main shocks, we observed a deepening of the base of the seismogenic regime, along with an increase of the seismicity rate within the

basement (Figs. 1A and 4C; SM8). We posit that this transient deepening was related to the polyphasic frictional rheology of the basement rocks. Following the main shocks ($M_w > 5.5$), an increase of loading rate (Fig. 1B) caused accelerating and self-decelerating aseismic creep in the weak phyllosilicate-rich matrix (Figs. 4A and 4B; Ellis and Stöckhert, 2004). The accelerated creep of the matrix transiently increased the stress at the edges and within the quartz-rich lenses. Small faults contained within single or neighboring lenses could thus reactivate, producing small cluster activity (Figs. 4A and 4D). In this interpretation, the post-main shock transient deepening of seismicity within the basement (Figs. 1B and 4C) resulted from a frictional aseismic-to-seismic transition within a rheologically heterogeneous deformation zone (e.g., Fagereng and Beall, 2021) rather than a strain rate-induced ductile-to-brittle switch (Sibson, 1989; Cheng and Ben-Zion, 2019). On a larger scale, the main shock-induced stress change caused an aftershock sequence in the whole basement that decayed inversely with time (Figs. 1B and 1C). The subsequent stress rate change caused a long-term response in the matrix (e.g., Toda et al., 2002; Ellis and Stöckhert, 2004), which induced the observed burst-type activity of the clusters (Fig. 2C).

The long-term accelerated creep within the phyllosilicate-rich basement is supported by interferometric synthetic aperture radar (InSAR) data and geodetic models highlighting tens of centimeters of afterslip in the months following the Norcia main shock at 10 km depth (Pousse-Beltran et al., 2020; Mandler et al., 2021). These

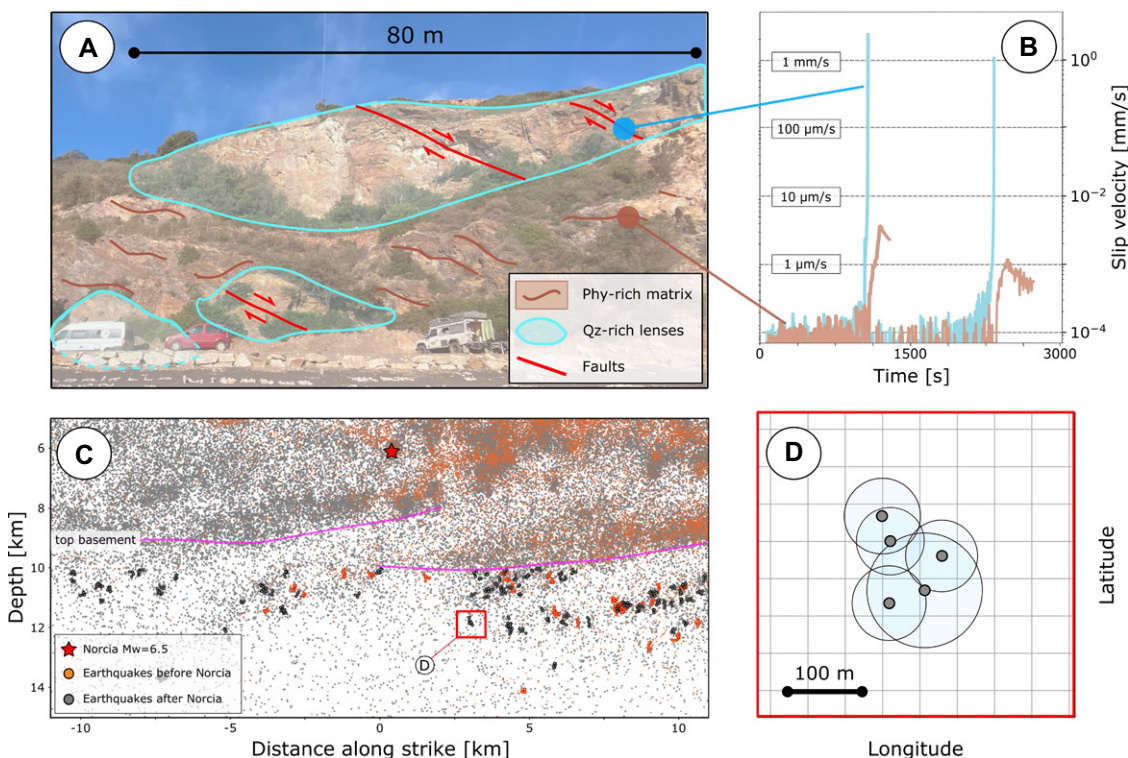


Figure 4. Road to integration. (A) Geological interpretation of selected outcrop of exhumed basement rocks (Elba Island). Phy—phyllosilicates; Qz—quartz. (B) Experimental results showing different styles of reactivation between matrix (aseismic) and lenses (seismic). (C) Geological cross section (trace of section in Fig. 1A) showing seismicity recorded 50 d before (orange dots) and after (gray dots) Norcia $M_w = 6.5$ main shock. Represented earthquakes are within 5 km of cross section. Clusters are highlighted in darker colors. (D) Plan view of selected cluster highlighting earthquakes with partially overlapping rupture area.

observations, together with the occurrence of basement seismicity in a large volume and in a relatively short time (Fig. 1C), suggest that this seismicity is consistent with stress-transfer processes modulated by the phyllosilicate-rich matrix. Our analysis highlights the fundamental role of structural and frictional heterogeneities in modulating the seismicity at the roots of the seismogenic zone. These results provide complementary and supporting evidence to the seismological observation of clusters of repeating earthquakes, which are interpreted as the result of rupture of discrete structures loaded by surrounding fault creep (Nadeau et al., 1994; Igarashi et al., 2003; Avouac, 2015; Uchida and Bürgmann, 2019).

ACKNOWLEDGMENTS

We thank M.R. Barchi and E. Carminati for fruitful discussions regarding the basement structures. This research was supported by European Research Council (ERC) grant 259256 GLASS and DPC to C. Collettini and ERC grant TECTONIC 835012 to C. Marone. Funding for G. Pozzi is provided by ERC grant FEAR 856559.

REFERENCES CITED

Anderlini, L., Serpelloni, E., and Belardinelli, M.E., 2016, Creep and locking of a low-angle normal fault: Insights from the Altotiberina fault in the Northern Apennines (Italy): *Geophysical Research Letters*, v. 43, p. 4321–4329, <https://doi.org/10.1002/2016GL068604>.

Avouac, J.P., 2015, From geodetic imaging of seismic and aseismic fault slip to dynamic modeling of the seismic cycle: *Annual Review of Earth and Planetary Sciences*, v. 43, p. 233–271, <https://doi.org/10.1146/annurev-earth-060614-105302>.

Barchi, M.R., Carboni, F., Michele, M., Ercoli, M., Giorgetti, C., Porreca, M., Azzaro, S., and Chiaraluce, L., 2021, The influence of subsurface geology on the distribution of earthquakes during the 2016–2017 Central Italy seismic sequence: *Tectonophysics*, v. 807, <https://doi.org/10.1016/j.tecto.2021.228797>.

Bedford, J.D., Faulkner, D.R., and Lapusta, N., 2022, Fault rock heterogeneity can produce fault weakness and reduce fault stability: *Nature Communications*, v. 13, 326, <https://doi.org/10.1038/s41467-022-27998-2>.

Brace, W.F., and Kohlstedt, D.L., 1980, Limits on lithospheric stress imposed by laboratory experiments: *Journal of Geophysical Research: Solid Earth*, v. 85, p. 6248–6252, <https://doi.org/10.1029/JB085iB11p06248>.

Cheng, Y., and Ben-Zion, Y., 2019, Transient brittle-ductile transition depth induced by moderate-large earthquakes in southern and Baja California: *Geophysical Research Letters*, v. 46, p. 11,109–11,117, <https://doi.org/10.1029/2019GL084315>.

Chiaraluce, L., Chiarabba, C., Collettini, C., Piccinini, D., and Cocco, M., 2007, Architecture and mechanics of an active low-angle normal fault: Alto Tiberina fault, northern Apennines, Italy: *Journal of Geophysical Research: Solid Earth*, v. 112, B10, <https://doi.org/10.1029/2007JB005015>.

Chiaraluce, L., Di Stefano, R., Tinti, E., Scognamiglio, L., Michele, M., Casarotti, E., Cattaneo, M., De Gori, P., Chiarabba, C., Monachesi, G., Lombardi, A., Valoroso, L., Latorre, D., and Marzotati, S., 2017, The 2016 Central Italy seismic sequence: A first look at the mainshocks, aftershocks, and source models: *Seismological Re-*

search Letters, v. 88, p. 757–771, <https://doi.org/10.1785/0220160221>.

Collettini, C., Tesi, T., Scuderi, M.M., Carpenter, B.M., and Viti, C., 2019, Beyond Byerlee friction, weak faults, and implications for slip behavior: *Earth and Planetary Science Letters*, v. 519, p. 245–263, <https://doi.org/10.1016/j.epsl.2019.05.011>.

Collettini, C., Barchi, M.R., De Paola, N., Trippetta, F., and Tinti, E., 2022, Rock and fault rheology explain differences between on fault and distributed seismicity: *Nature Communications*, v. 13, 5627, <https://doi.org/10.1038/s41467-022-33373-y>.

Ellis, S., and Stöckhert, B., 2004, Elevated stresses and creep rates beneath the brittle-ductile transition caused by seismic faulting in the upper crust: *Journal of Geophysical Research: Solid Earth*, v. 109, B05407, <https://doi.org/10.1029/2003JB002744>.

Essing, D., and Poli, P., 2022, Spatiotemporal evolution of the seismicity in the Alto Tiberina fault system revealed by a high-resolution template matching catalog: *Journal of Geophysical Research: Solid Earth*, v. 127, <https://doi.org/10.1029/2022JB024845>.

Fagereng, Å., and Beall, A., 2021, Is complex fault zone behaviour a reflection of rheological heterogeneity?: *Philosophical Transactions of the Royal Society A*, v. 379, <https://doi.org/10.1098/rsta.2019.0421>.

Fagereng, Å., and Sibson, R.H., 2010, Mélange rheology and seismic style: *Geology*, v. 38, p. 751–754, <https://doi.org/10.1130/G30868.1>.

Faulkner, D.R., Jackson, C.A.L., Lunn, R.J., Schlische, R.W., Shipton, Z.K., Wibberley, C.A.J., and Withjack, M.O., 2010, A review of recent developments concerning the structure, mechanics, and fluid flow properties of fault zones: *Journal of Structural Geology*, v. 32, p. 1557–1575, <https://doi.org/10.1016/j.jsg.2010.06.009>.

Giuntoli, F., and Viola, G., 2022, A likely geological record of deep tremor and slow slip events from a subducted continental broken formation: *Scientific Reports*, v. 12, 4506, <https://doi.org/10.1038/s41598-022-08489-2>.

Igarashi, T., Matsuzawa, T., and Hasegawa, A., 2003, Repeating earthquakes and interplate aseismic slip in the northeastern Japan subduction zone: *Journal of Geophysical Research: Solid Earth*, v. 108, 2249, <https://doi.org/10.1029/2002JB001920>.

Ikari, M.J., Marone, C., and Saffer, D.M., 2011, On the relation between fault strength and frictional stability: *Geology*, v. 39, p. 83–86, <https://doi.org/10.1130/G31416.1>.

Improta, L., Latorre, D., Margheriti, L., Nardi, A., Marchetti, A., Lombardi, A.M., Castello, B., Villani, F., Ciaccio, M.G., Mele, F.M., and Moretti, M., 2019, Multi-segment rupture of the 2016 Amatrice-Visso-Norcia seismic sequence (central Italy) constrained by the first high-quality catalog of early aftershocks: *Scientific Reports*, v. 9, 6921, <https://doi.org/10.1038/s41598-019-43393-2>.

Kanamori, H., and Anderson, D.L., 1975, Theoretical basis of some empirical relations in seismology: *Bulletin of the Seismological Society of America*, v. 65, p. 1073–1095, <https://doi.org/10.1785/BSSA0650051073>.

Lockner, D.A., Morrow, C., Moore, D., and Hickman, S., 2011, Low strength of deep San Andreas fault gouge from SAFOD core: *Nature*, v. 472, p. 82–85, <https://doi.org/10.1038/nature09927>.

Magistrale, H., 2002, Relative contributions of crustal temperature and composition to controlling the depth of earthquakes in southern California: *Geophysical Research Letters*, v. 29, p. 87-1–87-4, <https://doi.org/10.1029/2001GL014375>.

Mandler, E., Pintori, F., Gualandi, A., Anderlini, L., Serpelloni, E., and Belardinelli, M.E., 2021, Post-seismic deformation related to the 2016 Central Italy seismic sequence from GPS displacement time-series: *Journal of Geophysical Research: Solid Earth*, v. 126, <https://doi.org/10.1029/2021JB022200>.

Nadeau, R., Antolik, M., Johnson, P.A., Foxall, W., and McEvilly, T.V., 1994, Seismological studies at Parkfield III: Microearthquake clusters in the study of fault-zone dynamics: *Bulletin of the Seismological Society of America*, v. 84, p. 247–263, <https://doi.org/10.1785/BSSA0840020247>.

Pauselli, C., Gola, G., Mancinelli, P., Trumpy, E., Saccone, M., Manzella, A., and Ranalli, G., 2019, A new surface heat flow map of the Northern Apennines between latitudes 42.5 and 44.5 N: *Geothermics*, v. 81, p. 39–52, <https://doi.org/10.1016/j.geothermics.2019.04.002>.

Pialli, G., 1998, Results of the CROP3 Deep Seismic Reflection Profile: *Memorie della Società Geologica Italiana* 52, 657 p.

Pousse-Beltran, L., Socquet, A., Benedetti, L., Doin, M.P., Rizza, M., and d'Agostino, N., 2020, Localized afterslip at geometrical complexities revealed by InSAR after the 2016 Central Italy seismic sequence: *Journal of Geophysical Research: Solid Earth*, v. 125, <https://doi.org/10.1029/2019JB019065>.

Sibson, R.H., 1989, Earthquake faulting as a structural process: *Journal of Structural Geology*, v. 11, p. 1–14, [https://doi.org/10.1016/0191-8141\(89\)90032-1](https://doi.org/10.1016/0191-8141(89)90032-1).

Tan, Y.J., Waldhauser, F., Ellsworth, W.L., Zhang, M., Zhu, W., Michele, M., Chiaraluce, C., Beroza, C.G., and Segou, M., 2021, Machine-learning-based high-resolution earthquake catalog reveals how complex fault structures were activated during the 2016–2017 Central Italy sequence: *The Seismic Record*, v. 1, p. 11–19, <https://doi.org/10.1785/0320210001>.

Toda, S., Stein, R.S., and Sagiya, T., 2002, Evidence from the AD 2000 Izu islands earthquake swarm that stressing rate governs seismicity: *Nature*, v. 419, p. 58–61, <https://doi.org/10.1038/nature00997>.

Uchida, N., and Bürgmann, R., 2019, Repeating earthquakes: *Annual Review of Earth and Planetary Sciences*, v. 47, p. 305–332, <https://doi.org/10.1146/annurev-earth-053018-060119>.

Vidale, J.E., and Shearer, P.M., 2006, A survey of 71 earthquake bursts across southern California: Exploring the role of pore fluid pressure fluctuations and aseismic slip as drivers: *Journal of Geophysical Research: Solid Earth*, v. 111, B05312, <https://doi.org/10.1029/2005JB004034>.

Volpe, G., Pozzi, G., Carminati, E., Barchi, M.R., Scuderi, M.M., Tinti, E., Aldega, L., Marone, C., and Collettini, C., 2022, Frictional controls on the seismogenic zone: Insights from the Apenninic basement, central Italy: *Earth and Planetary Science Letters*, v. 583, <https://doi.org/10.1016/j.epsl.2022.117444>.

Vuan, A., Suga, M., Chiaraluce, L., and Di Stefano, R., 2017, Loading rate variations along a midcrustal shear zone preceding the Mw 6.0 earthquake of 24 August 2016 in central Italy: *Geophysical Research Letters*, v. 44, p. 12,170–12,180, <https://doi.org/10.1002/2017GL076223>.

Waldhauser, F., Michele, M., Chiaraluce, L., Di Stefano, R., and Schaff, D.P., 2021, Fault planes, fault zone structure and detachment fragmentation resolved with high-precision aftershock locations of the 2016–2017 Central Italy sequence: *Geophysical Research Letters*, v. 48, <https://doi.org/10.1029/2021GL092918>.

Printed in the USA